CFD ANALYSIS OF DRAG FORCES ACTING ON JACK-UP LEG CHORDS

Zhirong Shen, Kai Yu, Zhongfu Ge, Qing Yu*
American Bureau of Shipping

Zana Sulaiman, Henri van der Heiden, Hugo Hofstede
GustoMSC B.V.

* *corresponding author: qyu@eagle.org*

ABSTRACT

A comprehensive validation study of the CFD prediction of the drag forces acting on split-tube jack-up leg chords in steady incoming flows was performed. The study analyzed three jack-up leg chord models with different dimensions. Two commonly used CFD software packages, STAR-CCM+ and OpenFOAM were used in this study. Different turbulence models including RANS, DES, and LES were investigated by both software packages. A parametric study of various CFD simulation parameters for one selected chord was first performed to identify a specific simulation scheme that provided the most consistent prediction. The results indicate that the DES turbulence model can deliver the best performance for the present problem. A grid convergence study was also carried out, indicating good convergence at different heading angles. This simulation scheme was then applied to all the jack-up leg chord models at various heading angles. The drag forces calculated by this specific CFD analysis model agree well with the values by experiments and empirical method for predicting the drag force of split-tube chords, whereas they may deviate significantly with other CFD modeling schemes.

KEY WORDS: Jack-up leg, chord, CFD, STAR-CCM+, OpenFOAM, DDES, RANS, LES

INTRODUCTION

With significant advancements in computation algorithms, software tools, and high-performance computing capacities, Computational Fluid Dynamics (CFD) analysis has evolved from a research topic to a powerful tool for practical applications in the offshore and marine industry. The success of CFD applications also relies on rigorous validation processes which are critical to the development of CFD analysis procedures that can produce consistent and reproducible calculation results.

The use of CFD analysis for jack-up designs is relatively sporadic compared to other areas in the offshore industry. Common applications at present include wind loads on exposed structures and tow resistance calculations. Some attempts have been made to use CFD to determine the loads on jack-up legs, but the challenges remain for this specific application, which involves turbulent flows around a complex bluff body.

ABS and GustoMSC recently partnered to develop the best practices for CFD analyses of hydrodynamic loads on jack-up legs. Established standards including SNAME T&R 5-5A [1] and ISO 19905-1 [2] are widely accepted by the industry for the load analysis of typical truss legs and, most notably, leg chords. The main objective of this joint effort is the development of CFD analysis procedures that can provide a consistent load calculation of the jack-up legs, specifically for those with shapes out of the applicable range of existing standards.

Unlike circular cylinders and other regularly shaped objects, few CFD studies have been reported for jack-up chords. An early attempt was made by Smith et al. [3] to study the Lattice Boltzmann Method, which is a type of CFD analysis method using the discrete particle formulation, for its application to the wind load prediction on jack-up legs. Lee et al. [4, 5] investigated the hydrodynamic forces of jack-up legs with a single chord and bay units respectively. Both current and wave conditions were considered in the study. Sulaiman et al. [6] applied STAR-CCM+ in a study of the hydrodynamic forces on non-standard jack-up legs with T-shaped racks. Different configurations of the jack-up legs with T-shaped racks were investigated for both current and wave conditions. These previous studies on hydrodynamic load on the jack-up legs and chords focused on the application of the traditional Reynolds-Average Navier-Stokes (RANS) model. Part of the scope of work of the present study extended to the evaluation of the applicability of other models such as Detached Eddy

Simulation (DES) and Large Eddy Simulation (LES), which could produce results with higher fidelity and substantially more fluid details.

This paper presents the results of the first phase of the joint study focused on CFD analysis of drag forces acting on split-tube chords in steady incoming flows. For validation purposes, the CFD analysis was performed at model scale and results are compared with model test results and empirical approaches recommended by ISO 19905-1 [2]. Since the Reynolds number in this type of problem is relatively high ($\mathrm{Re} > 10^6$), the choice of turbulence models was critical. The performance of different turbulence models, including RANS, DES, and LES, as well as various modeling parameters such as grid size, time step, domain size, boundary conditions and integration method, were investigated through extensive parametric studies. The best set-up obtained through the parametric studies was further validated by a wide range of case studies involving a combination of three different jack-up leg chord models at seven heading angles.

MODEL TESTS

Three split-tube chord models were investigated for this study. The model geometries and model test data were collected and summarized in the MSC report [7]; the investigated models are model 1, model 6 and model 7. For each of these chord models, experimental measurements were carried out to measure the drag force acting on the chords.

In the large towing tank at the ship hydrodynamics laboratory of Delft University of Technology, model test experiments were performed to measure the current (drag) force acting on chord model 1 [8]. The measurements were performed at model scale at Reynolds number of 4×10^5 and on a section of the chord located below the still water level and above the tank bottom. It was mentioned that blockage effects due to the tank walls and free-surface disturbances during tow may influence the measured drag force. Therefore, corrections were applied to the drag coefficients to take the tank wall influence into account. However, based on the evaluation of the measurement accuracies, it was found that any measuring inaccuracy that might exist could not be excluded from the experiments.

The drag coefficients for the chord models 6 and 7 were obtained from the wind tunnel measurements carried out at the High Speed wind Tunnel (HST) of the Netherlands National Aerospace Laboratory (NLR) in Amsterdam [7]. The model size was chosen such that the sidewall blockage effects could be kept to a minimum. The measurements, for the chord models 6 and 7, were performed at Reynolds numbers of 1.6×10^6 and 1.9×10^6, respectively.

EMPIRICAL METHOD

The empirical method provided by ISO 19905-1 (Clause A.7.3.2.4) [2] was applied in this study as a reference for comparison. It is noted that the model test results [7, 8] have been considered in the assessment of the formulation of the empirical method. The drag coefficient of a split-tube chord can be estimated by:

$$C_{Di} = \begin{cases} C_{D0} & 0^o < \theta \leq 20^o \\ C_{D0} + (C_{D1} W/D - C_{D0}) \cdot sin^2[(\theta - 20^o)9/7] & 20^o < \theta \leq 90^o \end{cases}$$

where C_{D0} is the drag coefficient for a tubular design with appropriate roughness, θ is flow heading angle, W is the average width of the rack, and D is the reference dimension of the chord. The definitions of θ, W and D are illustrated in Figure 1. C_{D1} is the drag coefficient for flow normal to the rack, which is defined by,

$$C_{D1} = \begin{cases} 1.8 & W/D < 1.2 \\ 1.4 + 1/3(W/D) & 1.2 < W/D < 1.8 \\ 2.0 & 1.8 < W/D \end{cases}$$

GEOMETRY OF JACKUP LEG CHORDS FOR CFD MODELING

The geometric information and the flow conditions for the three selected chord models are listed in Table 1. Figure 1 illustrates the definitions of the principal dimensions, where D is the diameter of the chord, W is the average width of the rack; θ is the heading angle which is the angle between flow direction and plane of rack. The CFD model surfaces are assumed to be smooth to simplify the problem. The test models are considered to possess lab-quality smooth surfaces. The surface roughness of the tested model may have some effect on the test results, but the magnitude of such an effect is believed to be insignificant.

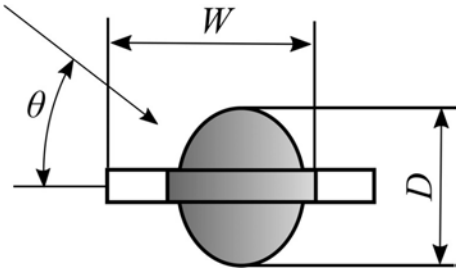

FIGURE 1 GEOMETRY OF A TYPICAL SPLIT TUBE CHORD

TABLE 1 INFORMATION ON JACK-UP CHORD MODELS

	Model 1	Model 6	Model 7
D (m)	0.3383	0.2541	0.2921
W (m)	0.4027	0.2865	0.3620
H (m)	0.674	0.674	0.674
Re (based on W)	1.9×10^6	1.6×10^6	1.9×10^6

The simulated drag forces are averaged over a period of time and the resultant mean forces normalized. The drag coefficient (C_d) is defined as,

$$C_d = \frac{F_d}{0.5\rho U^2 DH}$$

where F_d is the mean drag force, ρ is the fluid density, U is the inflow velocity, D is the diameter of the chord as defined in Figure 1, and H is the length of the chord. In this study, H is equal to four times the rack height. The value of D and H are listed in Table 1.

It is worth noting that the drag coefficient (C_d) is normalized by the average width (W) in the experimental report [7]. In order to have a consistent comparison, the values from the experiments are converted to those normalized by the chord diameter (D) correspondingly.

CFD MODELING

In this study, two commonly used CFD software packages, STAR-CCM+ and OpenFOAM, were used for the numerical study. The incompressible Navier-Stokes was applied as the governing equations in both software packages.

OpenFOAM

The open-source CFD library, OpenFOAM (v1812), was used for the numerical investigation. RANS, DES, and LES were applied to evaluate the effects of turbulence models. As for RANS, both Steady RANS (SRANS) and Unsteady RANS (URANS) were studied. SRANS ignores the time derivative term in the governing equations and uses the SIMPLE algorithm for pressure-velocity decoupling. For the unsteady simulations using URANS, the PISO algorithm was applied instead. Both SRANS and URANS use the classic $k-\omega\,SST$ turbulence model [9]. The LES model applies the one-equation Subgrid-Scale (SGS) model [10]. The DES model is a hybrid RANS/LES model. Among the DES model family, the Delayed DES based on the $k-\omega\,SST$

model[11] was selected. The results of SRANS can be used as the initial conditions for URANS, DES, and LES for faster convergence.

The second-order backward scheme was used for the temporal discretization scheme in all the unsteady simulations (i.e. except for SRANS). The gradient term was discretized by the least-squares method. The convection term applies a hybrid central difference (75%) and upwind (25%) scheme. The turbulence quantities were discretized by the central difference scheme.

Hexpress v7.2, which generates a hex-dominant mesh, was used to generate the mesh for all OpenFOAM simulations. An example of the surface mesh by Hexpress is illustrated in Figures 3 and 4. The first layer thickness of the near-wall mesh was determined by $y^+ \cong 1$ to fully resolve the sublayer region.

STAR-CCM+

The commercial software package STAR-CCM+ from Siemens [12] was also used to perform a numerical investigation into the performance of the Steady RANS, DES and LES turbulence models. For the steady RANS model, the closure of the Reynolds stress problem was achieved by means of the $k-\omega\ SST$ (Menter's Shear Stress Transport) turbulence model [9] with an all-y^+ wall treatment. For the DES model, the Delayed DES (DDES) model based on the $k-\omega\ SST$ turbulence model was also applied. The Wall-Adapting Large Eddy (WALE) Subgrid-Scale model was selected for the LES model.

The equations were spatially discretized using a second-order scheme and gradients were computed using a hybrid Gauss / Least Squares Method. For the unsteady DDES and LES simulations, the equations are temporally discretized using the implicit second-order scheme. Furthermore, the equations were iteratively solved in an uncoupled manner using the segregated flow solver. A predictor-corrector approach was invoked to link the momentum and continuity equations. The convection term in LES calculations utilized a bounded central differencing discretization, which blends a second-order central discretization with an upwind scheme. DDES calculations made use of a Hybrid second-order upwind/bounded central differencing discretization. In both cases, the default recommended settings for STAR-CCM+ were followed, which were based on a compromise between avoiding spurious numerical oscillations while also preventing the excessive dissipation of (turbulent) kinetic energy through the use of upwind schemes.

For all calculations, an unstructured hexa-dominant polyhedral mesh was generated in STAR-CCM+ by means of the trimmed mesh approach. Grid refinement was adopted around the chords and in the wake region to correctly solve the vortex shedding. In the immediate vicinity of the chord surface, a structured layer of prismatic cells was used to resolve the boundary layer. The height of the first prismatic cell and the total thickness of the prism layer were estimated to attain a y^+ value of 1. A surface growth rate of 1.25 was applied. Except for the boundary layer, all grid size properties were related to a base size. Depending on the case, most grids contained more than 10 million cells, which is considered a good compromise between accuracy and computational time based on sensitivity tests. Figure 2 illustrates examples of the applied computational grid with a detailed view of the surface mesh.

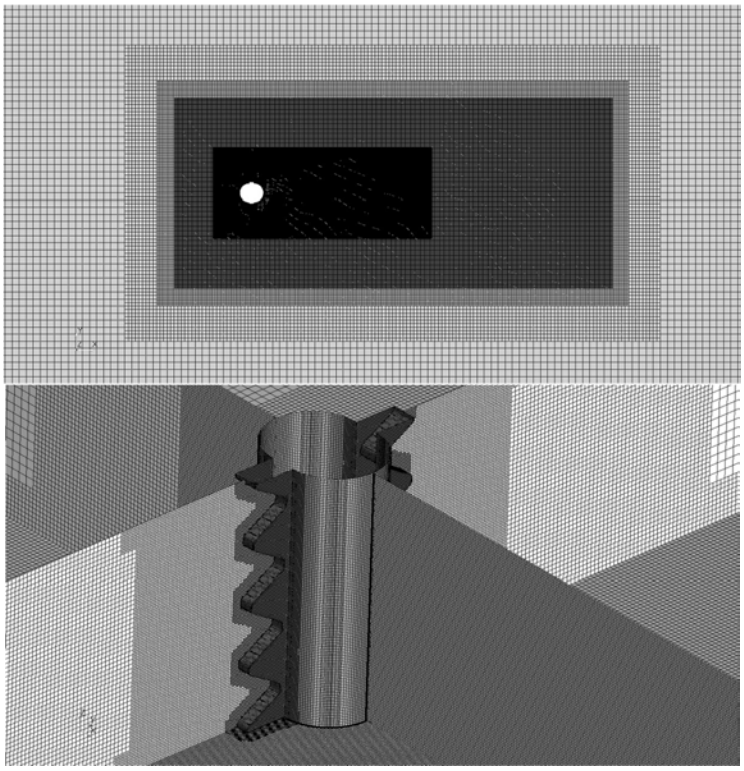

FIGURE 2. EXAMPLE OF THE APPLIED GRID IN STAR-CCM+ WITH A DETAILED VIEW OF THE SURFACE MESH.

RESULTS AND DISCUSSION

Grid Convergence Study Using OpenFOAM

A grid convergence study was carried out by OpenFOAM to evaluate and determine the proper mesh resolution for this type of problem. Three different grids with a refinement ratio of $\sqrt{2}$ in all x, y and z directions were created. The mesh was refined globally and systemically. The refinement procedure was performed as follows: First, the base mesh was refined according to the refinement ratio of $\sqrt{2}$. Second, the mesh was generated based on the refined base mesh created in the first step by continuously splitting the base mesh cells into smaller cells until designated criteria were satisfied. The diffusion level was adjusted in order to maintain the constant width transition region between the two refinement levels.

The three final generated grids are shown in Figure 3 The total number of cells range from 1.6 million to 7.2 million. A detailed view of the surface mesh is shown in Figure 4.

The grid convergence study was carried out for chord model 7 with the DDES turbulence model. Three heading angles of 0, 45 and 90 degrees were investigated. The results are illustrated in Figure 5. It can be seen from this figure that the drag force increases monotonically with increasing mesh resolution at 0 and 90 degrees. At the 45 degree heading, the drag force decreases monotonically with the refinement of the mesh. Monotonic convergence was achieved for all three heading angles although the convergence behavior was different. As a result, we chose the fine mesh for all the following simulations using OpenFOAM.

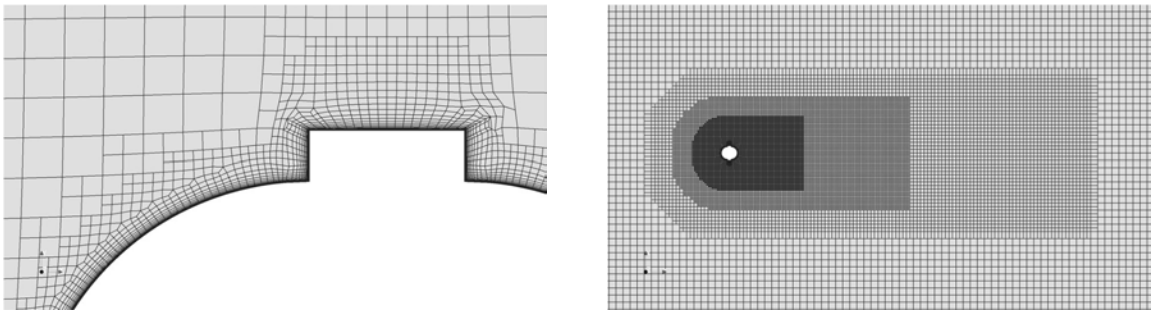

(a) Coarse Mesh (1.6 Million Cells)

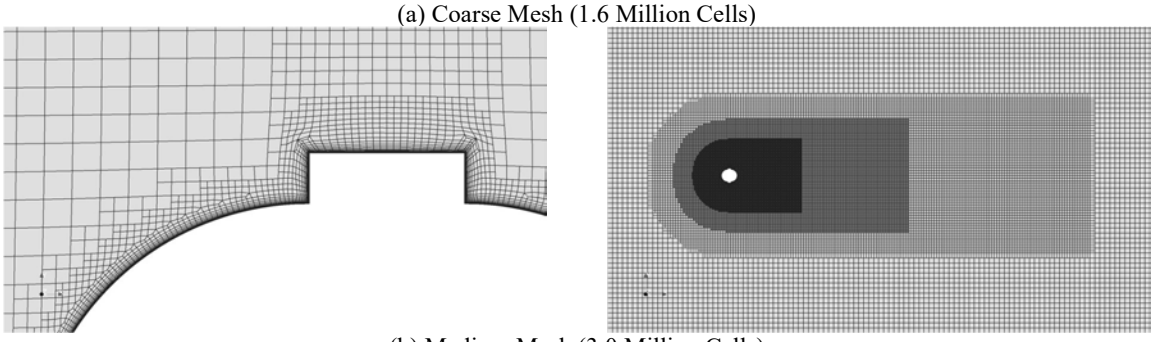

(b) Medium Mesh (3.0 Million Cells)

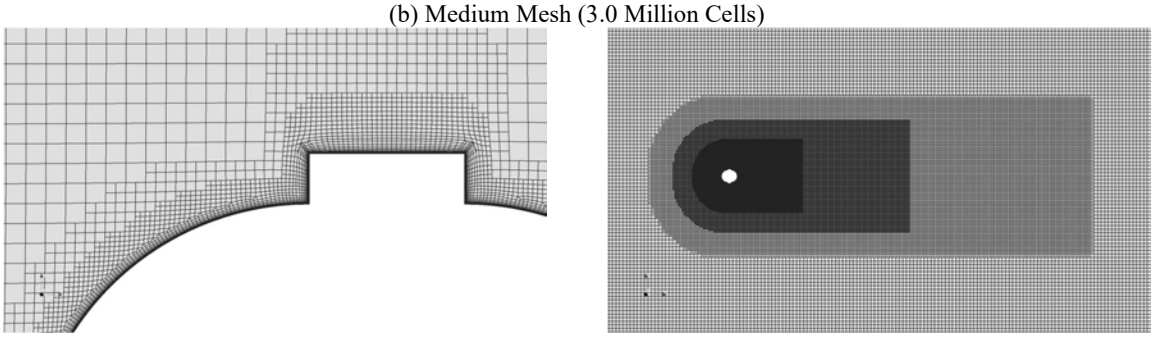

(c) Fine Mesh (7.2 Million Cells)

FIGURE 3 THREE SETS OF MESHES FOR GRID CONVERGENCE STUDY

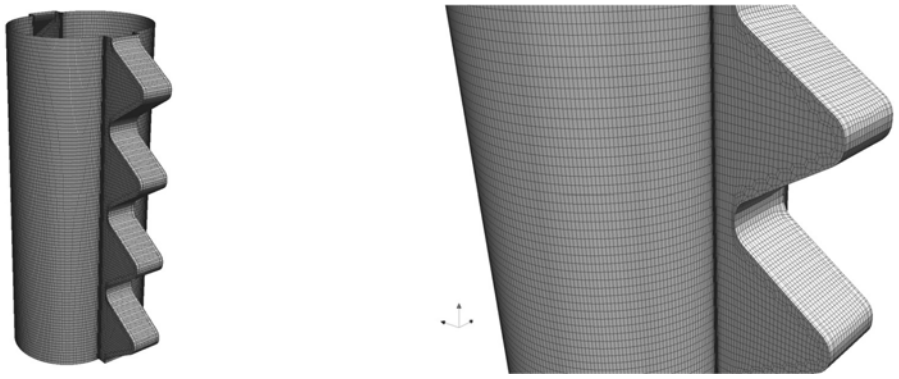

FIGURE 4 SURFACE MESH OF SPLIT-TUBE CHORD (COARSE MESH)

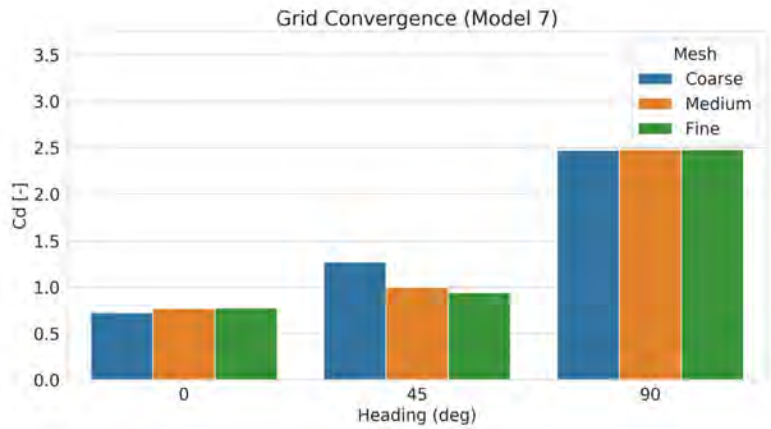

FIGURE 5 RESULTS OF GRID CONVERGENCE STUDY

Grid Convergence Study Using STAR-CCM+

A grid convergence study was carried out for the steady RANS calculations, using the same systematic refinement of the grid size as performed with OpenFOAM. In STAR-CCM+, this study was performed for the chord model 1. The coarse, medium and fine meshes contained 3.8 million, 9.9 million and 16.4 million cells, respectively. The drag coefficient results for the different grids are given in Figure 6. It can be seen from this figure that the steady RANS drag coefficients converge monotonically to a value of approximately 3.2. The calculated drag coefficient from the mesh of 9.9 million cells differs less than 2 percent from that of the fine mesh of 16.4 million cells. Therefore, it can be concluded that good grid convergence was achieved.

The steady RANS calculation results were used as an initial condition for the DDES and LES calculations for faster convergence. Since, in general, a fine mesh required for the DDES and LES calculations, the fine mesh of 16.4 million cells was applied in all the calculations to perform the comparative study of the three turbulence models.

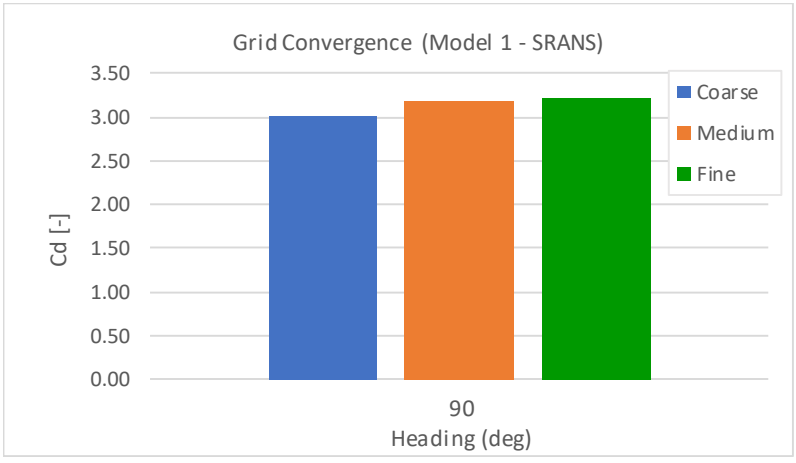

FIGURE 6 RESULTS OF GRID CONVERGENCE STUDY OBTAINED WITH STAR-CCM+

Comparative Study of Turbulence Models Using OpenFOAM

Chord model 7 was selected for the comparative study of turbulence models. Turbulence models SRANS, URANS, DDES and LES were investigated. Note that all the models have the same fine mesh of 7.2 million cells. The drag coefficients (C_d) obtained by the empirical method (ISO) and the Experimental Fluid Dynamics (EFD) data are used for comparison, as shown in Figure 7. The SRANS results in a close agreement at 0 and 45 degrees, but the discrepancy is more noticeable at 90 degrees. This indicates that the steady-state approach

might not be suitable for the unsteady problem studied here, despite the high efficiency of SRANS model. The result by URANS is underpredicted at 45 degrees but overpredicted at 90 degrees compared with the results from the ISO and EFD. Surprisingly, LES performed poorly in 0 and 90 degrees. After investigating the mesh quality, we found mesh cells with high non-orthogonality near the sharp edge of the chord rack, which caused significantly large negative pressure. This phenomenon indicated that LES is more sensitive to mesh quality than other models. LES can be practical for objects with regular shapes, such as circular cylinders, but for a more complex shape like split-tube chords, it is difficult to predict the results accurately by LES without applying significant mesh refinement.

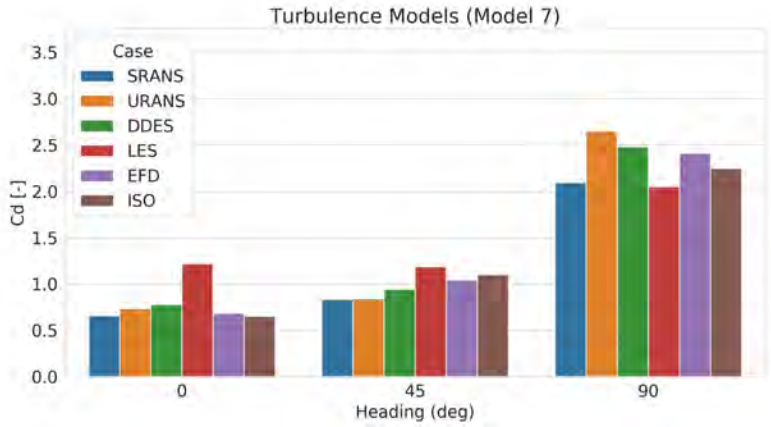

FIGURE 7 DRAG COEFFICIENTS FOR DIFFERENT TURBULENCE MODELS COMPARED WITH ISO AND EFD RESULTS.

Figure 8 illustrates the instantaneous vortex structures created using URANS, DDES, and LES respectively. The left column of Figure 8 shows the instantaneous iso-surface of Q, the second invariant of the velocity gradient tensor. The right column shows the instantaneous z-component of the vorticity. The URANS model shows a relatively coarse vortex even though the same mesh as for DDES and LES models is used. The DDES and LES models can capture significantly more details of vortex than URANS. The results illustrate a slight difference between DDES and LES in terms of the vortex: the vortex dissipates more quickly in the far-field in LES than DDES. This is because LES requires the refined mesh to resolve the small-scale vortex while DDES can switch to RANS when the mesh is coarse. Due to its hybrid nature, the DDES model can achieve a fairly good balance between computational cost and accuracy.

Among all the investigated turbulence models, DDES possesses the best trade-off among all three heading angles. It can overall achieve the closest comparison to the experimental data (EFD) as well as the empirical method (ISO). Compared with LES, DDES is a hybrid DES/LES method and it performs RANS simulation in the near-wall region, which is more tolerant with complex geometry and mesh quality than the pure LES method. Therefore, the DDES model is considered the most suitable model for the current problem among all the turbulence models investigated in this study.

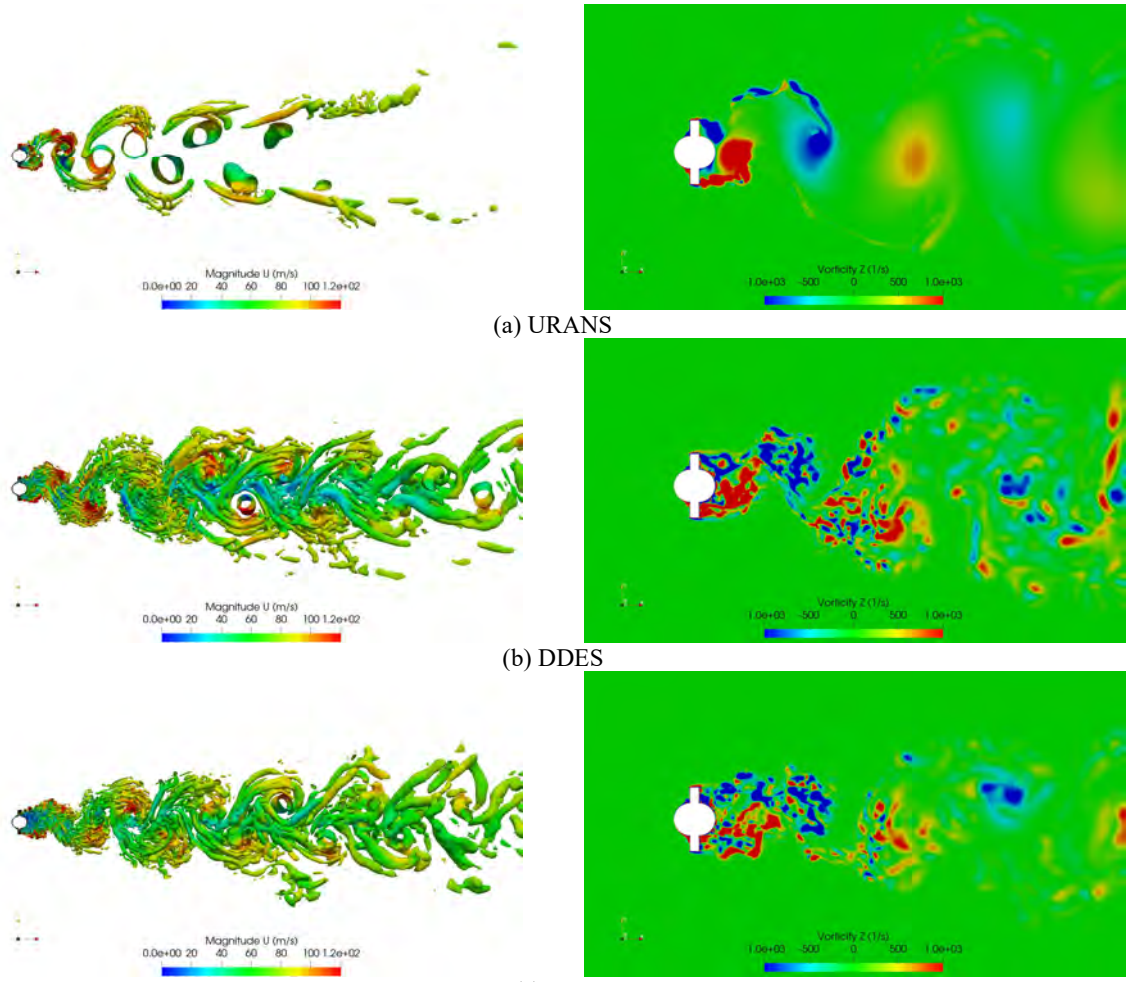

(a) URANS

(b) DDES

(c) LES

FIGURE 8 INSTANTANEOUS VORTEX STRUCTURES OF THREE DIFFERENT TURBULENCE MODELS (LEFT: ISO-SURFACE OF Q; RIGHT: Z-COMPONENT OF VORTICITY) FOR CHORD MODEL 7.

Comparative Study of Turbulence Models Using STAR-CCM+

A comparative study of turbulence models was carried out to assess the drag coefficient for each of the three chord models using STAR-CCM+. To limit the scope of the investigation, all presented calculations are performed for a heading angle of 90 degrees using the fine computational grid of 16.4 million cells. The CFD drag coefficient results obtained using steady RANS, DDES and LES models are presented in Figure 9 for the three considered chord models.

In agreement with the findings from the OpenFOAM calculations, the LES results deviated significantly from the EFD and ISO drag coefficients. This might be due to the fact that finer meshes are required for the LES calculations and further refinement of the mesh might be necessary to get more accurate results. The steady RANS calculations performed using STAR-CCM+ led to significantly higher drag coefficients for all the chord models, and was in this study the worst performing turbulence model. The DDES calculations systematically led to higher drag coefficients than obtained from EFD and ISO, but the results were closer to the EFD and ISO drag coefficients.

It should be noted that for chord model 7, the DDES results obtained using STAR-CCM+ were higher than those obtained using OpenFOAM for a heading angle of 90 degrees. However, it can be concluded from the results of the three applied turbulence models in STAR-CCM+ that the DDES calculations provided the best prediction of the drag coefficients with respect to the EFD and ISO results.

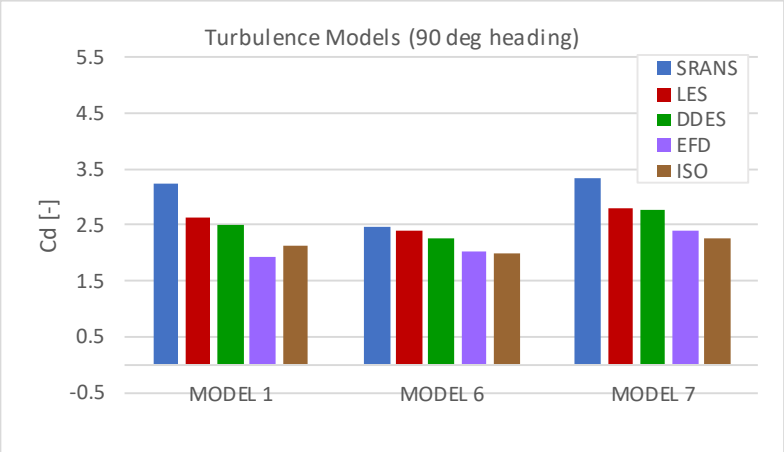

FIGURE 9 DRAG COEFFICIENTS FOR DIFFERENT TURBULENCE MODELS OBTAINED WITH STAR-CCM+, COMPARED WITH ISO AND EFD RESULTS.

Drag Force Curves for All Chord Models Calculated by OpenFOAM

The DDES model in OpenFOAM was selected to simulate all the jack-up leg chord models at different heading angles ranging from 0 to 90 degrees. The fine mesh (7.2 million cells) in the grid convergence study was applied. The same CFD setup except the inlet velocity was applied for all simulations.

Figures 10-12 show the predicted drag coefficients (C_d) from the CFD simulation DDES model and the comparison with the EFD and ISO results. In general, the CFD simulations using the DDES model achieved good accuracy. The C_d value for chord model 6 and chord model 7 were well predicted compared to EFD. For chord model 1, a notable discrepancy between DDES and EFD was found at a heading angle of 90 degrees. It is worth noting that the experiment for chord model 1 was done in the towing tank, while the tests for the chord models 6 and7 were performed in wind tunnels. The free surface in the towing tank experiment might have minor effects on the drag force. Moreover, as mentioned earlier, it was concluded from the towing tank experiments that measuring inaccuracy that might exist could not be excluded from the experiments. For all chord models, the C_d values at 0 degree were slightly higher than the values at 15 degrees.

These issues require further investigation in future work.

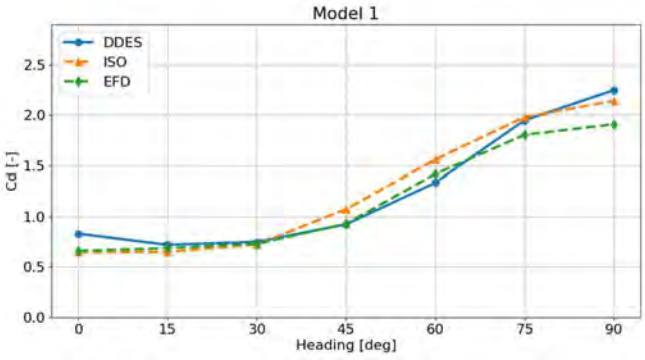

FIGURE 10 DRAG COEFFICIENTS FOR CHORD MODEL1 AT VARIOUS HEADING ANGLES

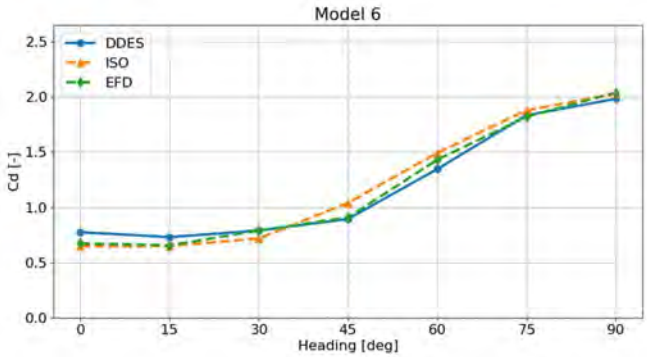

FIGURE 11 DRAG COEFFICIENTS FOR CHORD MODEL6 AT VARIOUS HEADING ANGLES

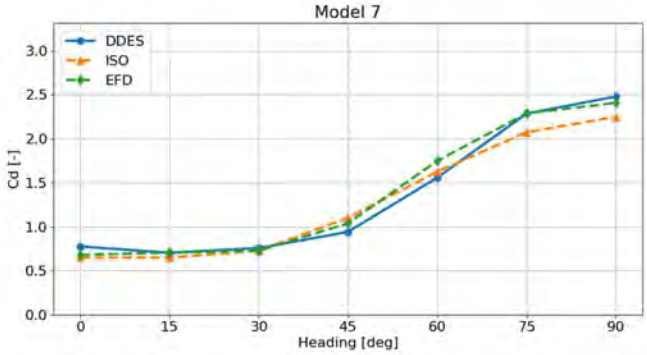

FIGURE 12 DRAG COEFFICIENTS FOR CHORD MODEL7 AT VARIOUS HEADING ANGLES

CONCLUSIONS

In this paper, a comprehensive validation study regarding CFD analysis of the drag forces of split-tube chords in steady incoming flows was performed. Three different chord models were investigated. Two commonly used CFD software packages in the offshore and marine industry, OpenFOAM and STAR-CCM+, were applied in this study. Parametric studies including a comparative study of different turbulence models and grid convergence were carried out to identify the best CFD model method for the present problem.

The RANS, DDES and LES models in OpenFOAM and STAR-CCM+ were evaluated for their application to the present problem. The RANS model appeared to be incapable of predicting the drag force accurately or consistently, and it generally produced relatively large errors. The DDES model shows a promising trend, and overall obtained the best accuracy. A grid convergence study was conducted using OpenFOAM, where the monotonic convergence was achieved at three heading angles (0, 45 and 90 degrees), indicating the grid resolution of the finest mesh is sufficient at least for the DDES model. The LES models showed significant deviation from the drag coefficients obtained from ISO and EFD, and generally performed worse than the DDES models. It was found that more refined meshes may be required for the LES calculations, which would significantly increase the computational cost. This conclusion holds for the results obtained using OpenFOAM as well as STAR-CCM+. Therefore, the DDES model was considered to be a reasonable balance between accuracy and computational cost.

Finally, the DDES turbulence model and the fine mesh of 7.2 million cells were applied for all three jack-up chord models at various heading angles in OpenFOAM. The DDES results for a heading angle of 90 degrees obtained using STAR-CCM+ were in general higher than the results obtained using OpenFOAM. However, it can be concluded that the CFD results demonstrated a good agreement with experimental results. The empirical method also provides a useful reference when evaluating the performance of the present CFD model.

This study provides an insight into the development of a suitable CFD simulation method for calculating the drag forces acting on jack-up leg chords. The scattering of analysis results due to using different CFD analysis approaches demonstrates the necessity of developing guidance on the best practice. In future work, further validation will be pursued for both current and wave loads as well as the application of the best practice to the jack-up leg or chord whose configurations are beyond the applicable range of existing empirical methods. It is expected that the validated CFD analysis method can become a valuable addition to the design toolbox for jack-ups.

REFERENCES

[1] SNAME, Guidelines for site specific assessment of mobile jack-up units, Technical & Research Bulletin 5-5A, 2008.

[2] ISO 19905-1, Petroleum and natural gas industries - Site-specific assessment of mobile offshore units – Part 1: Jack-ups, 2016.

[3] Smith P, Bailey J, Wu F. Virtual wind tunnel testing of jack-up legs. In: Proceedings of Eighth International Conference: The Jack-Up Platform – Design, Construction & Operation 2001.

[4] Lee SK, Yan D, Zhang B, Kang CW. Jack-up leg hydrodynamic load prediction-a comparative study of industry practice with CFD and model test results. In: Proceedings, Nineteenth International Offshore and Polar Engineering Conference (ISOPE) 2009.

[5] Lee SK, Yan D, Dong, Q, Hydrodynamic loads on leg chords of jack-up drilling units – A comparative study using CFD and industry practice, In: Proceedings, 4th PAAMES and AMEC2010, 2010.

[6] Sulaiman Z, Hofman A, Wallenburg C. Using CFD to Assess the Hydrodynamic Loads on Non-Standard Jack-up Leg Shapes. In: Proceedings, 27th International Ocean and Polar Engineering Conference (ISOPE) 2017.

[7] Largers, Morison Coefficients of Jack-Up legs, MSC, Report No: SP 8603-1505, 1990.

[8] Boon B., Keuning J. A., Test of MaTS Jack-up chord in towing tank, Delft University of Technology, Report OEMO 90/02, February 1990.

[9] Menter, FR, Kuntz, M and Langtry, R, Ten years of industrial experience with the SST turbulence model, Turbulence, heat and mass transfer, 2003, 4(1), 625-632.

[10] Yoshizawa A, Statistical theory for compressible turbulent shear flows, with the application to subgrid modeling. Physics of Fluids, 1986, 29(7):2152–2164.

[11] Gritskevich MS, Garbaruk AV, Schütze J, and Menter FR, Development of DDES and IDDES Formulations for the k-w Shear Stress Transport Model Flow, Turbulence and Combustion, 2012: 88(3):431–449.

[12] Siemens, STAR-CCM+ User Guide, v12.04.010, London, 2017.